Tomographic imaging of micrometer-sized optical and soft-x-ray beams

Hertz, H. M; Byer, R. L

Published in:
Optics Letters

DOI:
10.1364/OL.15.000396

1990

Tomographic imaging of micrometer-sized optical and soft-x-ray beams

H. M. Hertz* and R. L. Byer

Edward L. Ginzton Laboratory, Stanford University, Stanford, California 94305

Received October 2, 1989; accepted February 2, 1990

The knife-edge technique for measurements of micrometer-sized beams is extended to two-dimensional imaging by tomographic reconstruction of multiangular knife-edge data. Two-dimensional intensity distributions at optical (633-nm) and soft-x-ray (13.5-nm) wavelengths at the focal region of a Schwarzschild objective are presented. The resolution is limited by the 200-nm step size used in the data acquisition.

Determination of the spatial intensity distribution of micrometer-sized electromagnetic beams is of great importance in many fields, e.g., nonlinear optics, laser-induced damage studies, and scanning microscopy. Owing to its simplicity the knife-edge method has gained popularity for the measurement of Gaussian laser beams. In this Letter we present a tomographic technique that extends the applicability of the knife-edge method to measurements of beams with arbitrary intensity distributions. The method is demonstrated experimentally with images of the micrometer-sized intensity distribution in the focal region of a scanning soft-x-ray microscope,[1] at both optical and soft-x-ray wavelengths.

Several methods have been used for the measurement of focal spots of Gaussian laser beams: pinholes,[2] knife edges,[3] Ronchi gratings,[4] ribbons,[5] slits,[6] fluorescent films,[7] and a photothermal technique.[8] The knife-edge method has also been used for measurements on soft x rays[9] and electron beams.[10] Of the above methods only the pinhole method has demonstrated the potential to yield true two-dimensional (2-D) distributions. The fluorescent-film method has been extended to elliptical Gaussian beams, and the knife-edge method was recently extended to inverting arbitrary circular symmetric beams by use of the Abel transform.[11]

Computer-assisted tomography is a well-established technique for x-ray imaging in medicine and has applications in many other fields.[12] In general the technique permits the reconstruction of 2-D spatially resolved images from multiangular integrated measurements (projections). In the optical-wavelength region, tomography has been applied for imaging measurements of temperatures,[13] refractive indices,[14] species concentration,[15] and electrical fields.[16] In the x-ray region, in addition to the medical applications, absorption tomography has been performed on microscopic objects with x rays in the 10-keV range.[17]

By recording knife-edge scans at several angles through the beam and applying a tomographic algorithm to the data, we can reconstruct the 2-D image of the intensity distribution. Compared with the pinhole method, this tomographic technique avoids the use of small pinholes for high-resolution imaging, thus simplifying the alignment. Furthermore, it allows certain errors that occur during the scanning to be compensated for in the subsequent computer processing.

Figure 1 illustrates a knife edge cutting through an arbitrarily shaped beam with intensity distribution $F(x, y)$. It is clear that the measured edge response $f(x')$, i.e., the total transmitted intensity as a function of the knife-edge position x', is

$$f(x') = \int_{x'}^{\infty} \int_{-\infty}^{\infty} F(x, y)\mathrm{d}y\mathrm{d}x. \tag{1}$$

The derivative of Eq. (1) yields the line integrals

$$g(x') = -\int_{-\infty}^{\infty} F(x', y)\mathrm{d}y, \tag{2}$$

which constitute a projection. By rotating the scanning edge around the center of the coordinate system and acquiring the parallel-beam data for different angles θ, one obtains the multiangular projections necessary for the tomographic reconstruction. However, experimentally it is difficult to rotate an edge with micrometer precision with respect to the center of rotation. Furthermore, in our application (scanning soft-x-ray microscopy), that would involve the insertion of a rotator in the microscope, which is difficult mechanically. To facilitate the projection acquisition we instead used a 200-μm-diameter laser-drilled pin-

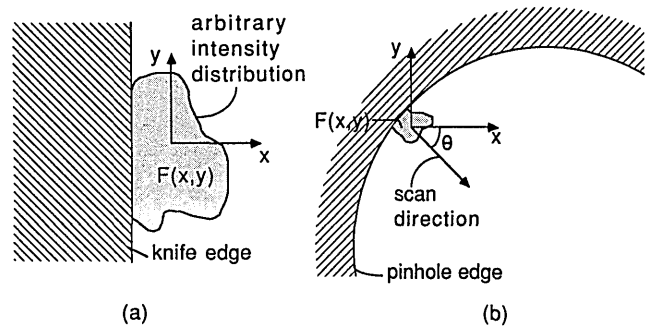

Fig. 1. Schematic illustrating (a) the knife-edge technique and (b) the use of a pinhole for multiangular projection acquisition.

0146-9592/90/070396-03$2.00/0

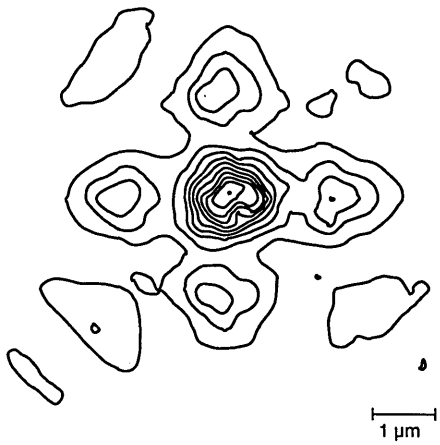

Fig. 2. Intensity distribution at the focal region of the Schwarzschild objective at $\lambda = 633$ nm. The contour intervals are 10% of peak intensity.

hole (Melles Griot) mounted on the existing motor-driven x–y–z stage in the microscope. As illustrated in Fig. 1(b), by driving the x and y stages at different rates one can scan the beam at different angles θ. This method greatly simplifies the alignment and the data acquisition while still not introducing large errors (errors are discussed below).

The scanning soft-x-ray microscope[1] utilizes a Schwarzschild objective to image a small soft-x-ray emitting source (a laser-produced plasma) onto the object to be studied. The F1.7 Schwarzschild objective has a focal length of 13.5 mm and demagnifies the source 100 times, producing a suitable (less than micrometer-sized) spot for scanning microscopy. The Schwarzschild objective consists of two nearly concentric spherical mirrors, which are coated with 40 layer pairs of Mo and Si for maximum normal-incidence reflection at $\lambda = 13.5$ nm. The top Mo layer also reflects well in the visible-wavelength region. Figure 2 shows the focal intensity distribution when we are imaging a visible source, a 50-μm pinhole illuminated with He–Ne radiation ($\lambda = 633$ nm), instead of the laser-produced plasma. The image is a 41 × 41 pixel picture, with each pixel being 200 nm × 200 nm. The strong sidelobes are due to diffraction by the four-armed spider, which holds the center mirror of the Schwarzschild objective. The FWHM of the central peak is 1.1 ± 0.1 μm, which compared well with the theoretically calculated FWHM for a diffraction-limited plane-wave system[18] (1.11 μm). The picture was reconstructed from four projections with the multiplicative algebraic reconstruction technique (MART) algorithm described below. Each projection had a resolution in the scanning of 140–200 nm (depending on θ). For testing purposes the focal spot was also reconstructed from eight projections, which yielded no additional spatial structure. In order to check the tomographic method further, a 1-μm-diameter pinhole was scanned line by line in 0.2-μm increments through the focal spot. The resulting image was compared with the tomographically reconstructed image, after the latter was smoothed to yield the same resolution as the lower-resolution 1-μm-pinhole image. The images agreed to within <4% of the peak image value.

Figure 3 shows the intensity distribution in the focal region of the Schwarzschild objective at $\lambda = 13.5$ nm. The soft-x-ray radiation was obtained by a laser-produced plasma on a rotating copper target, using a power of 20 mJ/pulse from a Quanta Ray DCR II Nd:YAG laser emitting 10-nsec pulses at 532 nm with a repetition rate of 10 Hz. The soft x rays were detected by an uncoated microchannel plate (Hamamatsu F2221-21S). The projection acquisition procedure was identical to that used for Fig. 2, with each data point being an average of 21 laser shots. Note the absence of diffraction sidelobes owing to the shorter wavelength. The FWHM is 0.8 μm, which is due mainly to the geometrical image of the estimated 100-μm-diameter plasma but also due to other sources discussed in Ref. 1. Reference 1 also discusses different methods to improve the resolution of the Schwarzschild x-ray microscope objective.

The resolution and quality of the reconstructed image are determined by several factors, of which the most important are roughness, curvature and thickness of the scanning edge, signal-to-noise ratio in the projections, and tomographic reconstruction artifacts.

The edge roughness of the laser-drilled pinholes was examined with a scanning electron microscope, which showed that the present pinholes had edge variations of approximately 50 nm. Sharper edges for higher-resolution measurements may be obtained by electron-beam lithography.[9] The error due to the curvature of the pinhole edge has to be examined for each beam size/pinhole diameter configuration. In our case, with a 200-μm-diameter pinhole in combination with 1–5-μm-diameter beams and a 200-nm step size, the errors are negligible. Furthermore, for low f-number objectives, such as the Schwarzschild objective examined here, the thickness of the scanning edge (here 13 μm) compared to the depth of focus (4 μm in the soft-x-ray case[1]) has to be examined. Fortunately the output diameter of the pinhole was slightly larger than the input diameter (206 and 200 μm, respectively), yielding a sufficiently sharp edge to probe only the focal region.

The most critical parameter for the image quality and resolution is the signal-to-noise ratio in the edge-response measurements since the projections used are the derivative of these measurements. Clearly, in or-

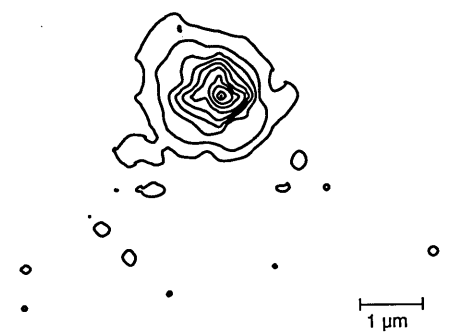

Fig. 3. Intensity distribution at the focal region of the Schwarzschild objective at $\lambda = 13.5$ nm showing a 0.8-μm FWHM spot size.

der to achieve a sufficient signal-to-noise ratio in the projections, the step size in numerical derivative of the slope in the edge response has to be large enough to overcome the noise. Thus the resolution in the image is limited by the signal-to-noise ratio. Mathematically this can be stated as

$$\Delta \geq \frac{N\sigma\sqrt{2}}{k}, \tag{3}$$

where Δ is the step size necessary to obtain a signal-to-noise ratio $\geq N$ for edge-response data with rms noise σ and slope k. Relation (3) assumes that the noise is Poisson distributed and that the step size is small compared with the total edge. It is obvious from relation (3) that the resolution required for a constant signal-to-noise ratio may vary along the scan since σ and k vary with position. Fortunately the required step size decreases for smaller beams since $\Delta \sim 1/k$, making measurements of small beams possible even in the existence of reasonable noise. The experimental measurements confirm relation (3). In the x-ray case we assumed that the signal-to-noise ratio in the projections should be greater than 5, which with a maximum slope of $0.6/\mu$m and maximum noise $\sigma_{max} = 0.01$ (arbitrary intensity units) results in a step size greater than 0.12 μm. The relation between noise in the projections and noise in the reconstructed picture has been discussed by many authors.[19]

In order to reduce the time for data acquisition and tomographic reconstruction, the focal-spot intensity distributions in the microscope were reconstructed from few projections (<10). Reconstruction from few projections requires a tomographic algorithm suited for the specific object to be reconstructed. In this Letter a modified MART algorithm[16] is used. Simulations show that the modified MART algorithm behaves well for reconstruction of smooth objects. However, when used for reconstruction of sharp edges it may yield erroneous results. For smoothly varying objects, such as the intensity distribution in diffraction-limited or reasonably aberrated systems, the reconstructions are stable even for as few as two or three projections.[15] Naturally reconstruction from so few projections yields limited spatial resolution. The dependence of the spatial resolution on the number of parallel rays and projection angles is described in Ref. 16. Because of the small number of projections used in this study, in principle high-frequency details may be lost, although that is unlikely with the types of objects imaged here. From simulations we estimate the reconstruction errors in the images presented here to be less than 5% of the maximum intensity. From the discussion above and the control measurements, the total errors in the images presented here are estimated to be 5–10% of the peak value.

In conclusion, we have described a simple tomographic imaging method to determine the intensity distribution of micrometer-sized beams and have demonstrated the method at both optical and soft-x-ray wavelengths. The method is easily incorporated into any scanning system. The resolution is ultimately limited by the knife-edge roughness, but in reality signal-to-noise ratio considerations are also a constraint. Since many of the above-mentioned conventional techniques for measuring Gaussian beam parameters may produce line integral measurements, they may also be extended to 2-D imaging by using the tomographic technique presented in this Letter. The approach described and demonstrated here may find practical use in the growing field of x-ray imaging in both telescopic and microscopic applications.

The authors gratefully acknowledge the generous assistance of John Trail. This project was financed by the National Science Foundation, the Swedish Natural Science Research Council, and the Sweden–America Foundation.

* Present address, Department of Physics, Lund Institute of Technology, P.O. Box 118, S-22100 Lund, Sweden.

References

1. J. A. Trail, "A compact soft x-ray microscope," Ph.D. dissertation (Stanford University, Stanford, Calif., 1989); J. A. Trail and R. L. Byer, Opt. Lett. **14**, 539 (1989).
2. P. J. Shayler, Appl. Opt. **17**, 2673 (1978).
3. A. H. Firester, M. E. Heller, and P. Sheng, Appl. Opt. **16**, 1971 (1977).
4. B. Cannon, T. S. Gardner, and D. K. Cohen, Appl. Opt. **25**, 2981 (1986).
5. A. Yoshida and T. Asakura, Opt. Laser Technol. **8**, 273 (1976).
6. R. L. McCally, Appl. Opt. **23**, 2227 (1984).
7. A. H. Stolpen, C. S. Brown, and D. E. Golan, Appl. Opt. **27**, 4414 (1988).
8. K. Williams, P. Glezen, and R. Gupta, Opt. Lett. **13**, 740 (1988).
9. H. Rarback, D. Shu, S. C. Feng, H. Ade, J. Kirz, I. McNulty, D. P. Kern, T. H. P. Chang, Y. Vladimirsky, N. Iskander, D. Attwood, K. McQuaid, and S. Rothman, Rev. Sci. Instrum. **59**, 52 (1988).
10. E. Oho, T. Sasaki, K. Adachi, and Koichi Kanaya, J. Electron. Microsc. Technol. **2**, 463 (1985).
11. R. M. O'Connell and R. A. Vogel, Appl. Opt. **26**, 2528 (1987).
12. G. T. Herman, ed., Special issue on computerized tomography, Proc. IEEE **71**, 291–435 (1983).
13. H. M. Hertz, Opt. Commun. **54**, 131 (1985).
14. G. W. Faris and R. L. Byer, Science **238**, 1700 (1987); G. W. Faris and H. M. Hertz, Appl. Opt. **28**, 4662 (1989).
15. H. M. Hertz and G. W. Faris, Opt. Lett. **13**, 351 (1988).
16. H. M. Hertz, Appl. Opt. **25**, 914 (1986).
17. B. P. Flannery, H. W. Deckman, W. G. Roberge, and K. L. D'Amico, Science **237**, 1439 (1987).
18. G. W. Faris, "Quantitative optical tomographic imaging of fluid flows and flames," Ph.D. dissertation (Stanford University, Stanford, Calif., 1986).
19. K. E. Bennet and R. L. Byer, J. Opt. Soc. Am. A **3**, 624 (1986), and references therein.